7564 *Inorg. Chem.* **2009**, *48*, 7564–7575
DOI: 10.1021/ic9001835

Inorganic Chemistry
Article

Mechanistic Study of $LiNH_2BH_3$ Formation from $(LiH)_4$ + NH_3BH_3 and Subsequent Dehydrogenation

Tae Bum Lee and Michael L. McKee*

Department of Chemistry and Biochemistry, Auburn University, Auburn, Alabama 36849

Received January 28, 2009

The formation of $LiNH_2BH_3$ from $(LiH)_4$ and NH_3BH_3 and the subsequent dehydrogenation have been studied computationally at the CCSD(T)/6-311++G(3d,2p)//MP2/6-311++G(2d,p) level. A cubic unit of $(LiH)_4$ is predicted to react readily with NH_3BH_3 to form $LiNH_2BH_3$ plus H_2. The $(LiH)_4$ tetramer enables dehydrogenation through the exchange of a hydride vertex of $(LiH)_4$ and $NH_2BH_3^-$ where $NH_2BH_3^-$ is formed when the hydride vertex of $(LiH)_4$ abstracts a proton from NH_3. The free energy of activation for loss of H_2 is reduced from 37.2 kcal/mol in NH_3BH_3 to 11.0 kcal/mol in $(LiH)_4$ + NH_3BH_3. Further, H_2 elimination from the $(LiNH_2BH_3)_2$ dimer is predicted to be much easier than from the monomer which may suggest a cooperative H_2-loss mechanism is possible in solid $LiNH_2BH_3$. While two molecules of H_2 can be lost reversibly from $(LiNH_2BH_3)_2$, loss of further H_2 molecules is more difficult but could occur if the lattice energy stabilization accompanying H_2 loss is sufficiently large.

Introduction

Hydrogen is ubiquitous, but bottling hydrogen may be the most challenging step for a hydrogen economy because the low density (and boiling point) of H_2 makes it difficult to store in compressed or liquefied form. Ammoniaborane (NH_3BH_3) is attracting a great deal of attention as a chemical storage system. It contains 19.6 wt % of H_2, which is larger than the 9.0 wt % target set by the U.S. Department of Energy for 2015.[1] Unlike CH_3CH_3, the first dehydrogenation of the NH_3BH_3 molecule is exothermic because of the conversion of an N−B dative bond into an N=B double bond.[2,3] However, this exothermic character vanishes as more hydrogen is generated since aminoborane ($H_2N{=}BH_2$) and iminoborane (HN≡BH), which have multiple bonds between nitrogen and boron, become endothermic for hydrogen release.[2] In terms of reversibility, NH_3BH_3 still requires further study to improve sustainable hydrogen storage systems. By using solid state quantum simulation, Miranda and Ceder[4] showed that dehydrogenation from both the polymeric ammoniaborane and cyclotriborazane were exothermic (approximately −10 kcal/mol), implying that rehydrogenation may be difficult at moderate H_2 pressures. Thus, the full amount of hydrogen in NH_3BH_3 may not be available as a relevant energy source. Some recent studies have attempted to improve hydrogen generation from NH_3BH_3 through a catalytic process.[3,5−8] However, these storage systems, which need solvent or catalyst, have a significantly lower storage capacity.

Meanwhile, $LiH/LiNH_2$ mixture and their derivatives are also attracting attention as hydrogen storage systems,[9−14] and several mechanistic studies have appeared.[14−16] Typically,

*To whom correspondence should be addressed. E-mail: mckee@chem.auburn.edu.

(1) (a) Marder, T. B. *Angew. Chem., Int. Ed.* **2007**, *46*, 8116. (b) Hamilton, C. W.; Baker, T.; Staubitz, A.; Manners, I. *Chem. Soc. Rev.* **2009**, *38*, 279.
(2) Dixon, D. A.; Gutowski, M. *J. Phys. Chem. A* **2005**, *109*, 5129.
(3) Staubitz, A.; Besora, M.; Harvey, J. N.; Manners, I. *Inorg. Chem.* **2008**, *47*, 5910.
(4) Miranda, C.; Ceder, G. *J. Chem. Phys.* **2007**, *126*, 184703.
(5) Cheng, F.; Ma, H.; Li, Y.; Chen, J. *Inorg. Chem.* **2007**, *46*, 788.
(6) Allouti, F.; Siebert, W.; Himmel, H.-J. *Inorg. Chem.* **2008**, *47*, 7631.
(7) (a) Peng, B.; Chen, J. *Energy Environ. Sci.* **2008**, *1*, 479. (b) Chen, P.; Zhun, M. *Mater. Today* **2008**, *11*, 36.
(8) (a) Staubitz, A.; Soto, P. A.; Manners, I. *Angew. Chem., Int. Ed.* **2008**, *47*, 6212. (b) Kalidindi, S. B.; Indirani, M.; Jagirdar, B. R. *Inorg. Chem.* **2008**, *47*, 7424.
(9) (a) Chen, P.; Xiong, Z.; Luo, J.; Lin, J.; Tan, K. L. *Nature* **2002**, *420*, 302. (b) Chen, P.; Xiong, Z.; Yang, L.; Wu, G.; Luo, W. *J. Phys. Chem. B* **2006**, *110*, 14221. (c) Chen, P.; Xiong, Z.; Luo, J.; Lin, J.; Tan, K. L. *J. Phys. Chem. B* **2003**, *107*, 10967.
(10) (a) Leng, H. Y.; Ichikawa, T.; Hino, S.; Hanada, N.; Isobe, S.; Fujii, H. *J. Phys. B.* **2004**, *108*, 8763. (b) Isobe, S.; Ichikawa, T.; Hino, S.; Fujii, H. *J. Phys. Chem. B* **2005**, *109*, 14855. (c) Hanada, N.; Ichikawa, T.; Fujii, H. *J. Phys. Chem. B* **2005**, *109*, 7188. (d) Leng, H.; Ichikawa, T.; Fujii, H. *J. Phys. Chem. B* **2006**, *110*, 12964.
(11) (a) Shaw, L. L.; Ren, R.; Markmaitree, T.; Osborn, W. *J. Alloys Compd.* **2008**, *448*, 263. (b) Ortiz, A. L.; Osborn, W.; Markmaitree, T.; Shaw, L. L. *J. Alloys Compd.* **2008**, *454*, 297.
(12) (a) Wu, H. *J. Am. Chem. Soc.* **2008**, *130*, 6515. (b) Baldé, C. P.; Hereijgers, B. P. C.; Bitter, J. H.; de Jong, K. P. *J. Am. Chem. Soc.* **2008**, *130*, 6761.
(13) Li, L.; Yao, X.; Sun, C.; Du, A.; Cheng, L.; Zhu, Z.; Yu, C.; Zou, J.; Smith, S. C.; Wang, P.; Cheng, H.-M.; Frost, R. L.; Lu, G. Q. *Adv. Funct. Mater.* **2009**, *19*, 265.
(14) (a) Shaw, L. L.; Osborn, W.; Markmaitree, T.; Wan, X. *J. Power Sources* **2008**, *177*, 500. (b) Ichikawa, T.; Hanada, N.; Isobe, S.; Leng, H. Y.; Fujii, H. *J. Phys. Chem. B* **2004**, *108*, 7887.
(15) Kar, T.; Scheiner, S.; Li, L. *THEOCHEM* **2008**, *857*, 111.
(16) Aguey-Zinsou, K.-F.; Yao, J.; Guo, Z. X. *J. Phys. Chem. B* **2007**, *111*, 12531.

 Published on Web 07/10/2009

Table 1. Reported H_2 wt % for the Thermal Decomposition from NH_3BH_3 + LiH[a]

decomposition	Xiong et al.[b]	Kang et al.[c]
loss of 1st H_2	5.2 wt % at 90 °C	5.2 wt % at 100 °C
loss of 2nd H_2	5.2 wt % at 90 °C	5.2 wt % at 100 °C
loss of 3rd H_2	5.2 wt % at 90 °C	4.1 wt % at 200 °C[d]

[a] Kang et al. used NH_3BH_3 + LiH as their reference to calculate H_2 wt % while Xiong et al. used $LiNH_2BH_3$ to report H_2 wt %. Thus, the value of 10.9 wt % reported by Xiong et al. corresponds to the 2nd and 3rd dehydrogenation in this table with $LiNH_2BH_3$ as the reference. [b] Reference 24. [c] Reference 26. [d] Calculated from the reported reaction of NH_3BH_3 + LiH → $LiNBH_{1.4}$ + $2.8H_2$. The isothermal decomposition behavior was not reported at 200 °C.

dehydrogenations in these systems are achieved through a ball-milling process, which does not require a solvent for operation. However, high thermal stability limits their use as a practical storage system. Many attempts have been made to lower the thermodynamic barriers of these hydride or amide derivatives through high-pressure polymorphism,[17] self-catalyzing material,[18] mixed alkali metal,[19] partial substitution of Li by K or Mg,[20] vacancies on the surface,[21] autocatalysis of NH_2BH_2,[22] and N-heterocyclic carbene[23] but still only partial successes have been reported.

Recently, Xiong et al.[24] reported a new storage system using ball milling of NH_3BH_3 and LiH powder (Table 1), through formation of a lithium amidoborane ($LiNH_2BH_3$) crystal. This process generates about 15.6 wt % of hydrogen (NH_3BH_3 + LiH → LiN≡BH + $2H_2$) at 90 °C which is a milestone for practical application of chemical storage, since polymer electrolyte membrane (PEM) fuel cell are limited by this operation temperature.[25] Kang et al.[26] used a similar temperature (100−120 °C) to achieve a 10.4 wt % dehydrogenation from a ball-milling process (Table 1). However, they reported that a higher temperature was required to reach the final product ($LiNBH_{1.4}$) which would correspond to a total wt % of 14.5. Thus, the two experimental studies report very similar results for the loss of the first two hydrogen molecules, but differ on the loss of the third hydrogen. In both studies, $LiNH_2BH_3$ does not generate borazine derivatives, which are undesirable byproduct for hydrogen storage.

Typically, NH_3BH_3, which tends to hydrolyze in acid (a process catalyzed by metals or promoted by solid acids), is very stable in neutral or basic aqueous solution.[1] Dixon and co-workers have suggested several catalytic processes through Lewis acid BH_3,[27] alane,[28] acid initiation of NH_3BH_3,[29] $(NH_3BH_3)_2$,[30] and ammonia triborane.[31] Interestingly, LiH and NH_3BH_3 mixture can generate three molar equivalents of H_2 without additional catalyst, an advantage since the catalyst would lower the wt % capacity of H_2 storage. Here, a thorough study of the mechanism of $LiNH_2BH_3$ formation and its subsequent dehydrogenation is presented based on ab initio computational quantum chemistry where the formation of $LiNH_2BH_3$ and the number of reversible dehydrogenation steps available from its decomposition is explored. Hopefully, this study can provide clues for the next advance of hydrogen storage, either through solid-state dehydrogenation or its catalytic promotion.

Computational Methods

Because of the systematic underestimation of reaction barrier heights by density functional theory (DFT) and overestimation of barrier heights by the MP2 formalism, all stationary points are calculated at the CCSD(T)/6-311++G(3d,2p)//MP2/6-311++G(2d,p) level using the Gaussian03 package.[32] Simplified intrinsic reaction coordinates (IRC) are used to confirm the identity of reactant and product from a transition state. The nature of the stationary points was determined with vibrational analysis at the MP2 level. Zero-point energies, heat capacity corrections, and $T\Delta S$ contributions at the MP2/6-311++G(2d,p) level were combined with single-point energies at the CCSD(T)/6-311++G(3d,2p) level to yield free energies at 298 K. This level of theory is expected to yield a potential energy surface within about 1 kcal/mol of the complete basis set limit.[30] Unless otherwise indicated energy values in the text will be free energies at 298 K. Figures will present relative free energies at 298 K followed by enthalpies at 298 K in parentheses.

Results

The reaction of NH_3BH_3(s) + LiH(s) in the ball-milling process at 90 °C releases one mole of H_2 per mole from a 1:1 mixture of NH_3BH_3 and LiH (eq 1).[24] NaH, which has the same ability to generate hydrogen through the formation of

(17) Filinchuk, Y.; Chernyshov, D.; Nevidomskyy, A.; Dmitriev, V. *Angew. Chem., Int. Ed.* **2008**, *47*, 529.
(18) Yang, J.; Sudik, A.; Siegel, D. J.; Halliday, D.; Drews, A. D.; Carter, R. O.; Wolverton, C.; Lewis, G. J.; Sachtler, J. W.; Low, J. J.; Faheem, S. A.; Lesch, D. A.; Ozolinš, V. *Angew. Chem., Int. Ed.* **2008**, *47*, 882.
(19) Nickels, E. A.; Jones, M. O.; David, W. I. F.; Johnson, S. R.; Lowton, R. L.; Sommariva, M. S.; Edwards, P. P. *Angew. Chem., Int. Ed.* **2008**, *47*, 2817.
(20) Zhang, C.; Alavi, A. *J. Phys. Chem. B* **2006**, *110*, 7139.
(21) Du, A. J.; Smith, S. C.; Yao, X. D.; Lu, G. Q. *J. Phys. Chem. C* **2007**, *111*, 12124.
(22) Zimmerman, P. M.; Paul, A.; Zhang, Z.; Musgrave, C. B. *Inorg. Chem.* **2009**, *48*, 1069.
(23) (a) Zimmerman, P. M.; Paul, A.; Zhang, Z.; Musgrave, C. B. *Angew. Chem., Int. Ed.* **2009**, *48*, 2201. (b) Zimmerman, P. M.; Paul, A.; Musgrave, C. B. *Inorg. Chem.* **2009**, *48*, 5418.
(24) Xiong, Z.; Yong, C. K.; Wu, G.; Chen, P.; Shaw, W.; Karkamkar, A.; Autrey, T.; Jones, M. O.; Johnson, S. R.; Edwards, P. P.; David, W. I. F. *Nat. Mater.* **2008**, *7*, 138.
(25) Benedetto, S. D.; Carewska, M.; Cento, C.; Gislon, P.; Pasquali, M.; Scaccia, S.; Prosini, P. P. *Thermochim. Acta* **2006**, *441*, 184.
(26) Kang, X.; Fang, Z.; Kong, L.; Cheng, H.; Yao, X.; Lu, G.; Wang, P. *Adv. Mater.* **2008**, *20*, 2756.
(27) Nguyen, M. T.; Nguyen, V. S.; Matus, M. H.; Gopakumar, G.; Dixon, D. A. *J. Phys. Chem. A* **2007**, *111*, 679.
(28) Nguyen, V. S.; Matus, M. H.; Ngan, V. T.; Nguyen, M. T.; Dixon, D. A. *J. Phys. Chem. C* **2008**, *112*, 5662.
(29) Stephens, F. H.; Baker, R. T.; Matus, M. H.; Grant, D. J.; Dixon, D. A. *Angew. Chem., Int. Ed.* **2007**, *46*, 746.
(30) Nguyen, V. S.; Matus, M. H.; Grant, D. J.; Nguyen, M. T.; Dixon, D. A. *J. Phys. Chem. A* **2007**, *111*, 8844.
(31) Nguyen, V. S.; Matus, M. H.; Nguyen, M. T.; Dixon, D. A. *J. Phys. Chem. C* **2007**, *111*, 9603.
(32) Frisch, M. J., Trucks G. W.; Schlegel, H. B.; Scuseria, G. E.; Robb, M. A.; Cheeseman, J. R.; Montgomery, Jr., J. A.; Vreven, T.; Kudin, K. N.; Burant, J. C.; Millam, J. M.; Iyengar, S. S.; Tomasi, J.; Barone, V.; Mennucci, B.; Cossi, M.; Scalmani, G.; Rega, N.; Petersson, G. A.; Nakatsuji, H.; Hada, M.; Ehara, M.; Toyota, K.; Fukuda, R.; Hasegawa, J.; Ishida, M.; Nakajima, T.; Honda, Y.; Kitao, O.; Nakai, H.; Klene, M.; Li, X.; Knox, J. E.; Hratchian, H. P.; Cross, J. B.; Bakken, V.; Adamo, C.; Jaramillo, J.; Gomperts, R.; Stratmann, R. E.; Yazyev, O.; Austin, A. J.; Cammi, R.; Pomelli, C.; Ochterski, J. W.; Ayala, P. Y.; Morokuma, K.; Voth, G. A.; Salvador, P.; Dannenberg, J. J.; Zakrzewski, V. G.; Dapprich, S.; Daniels, A. D.; Strain, M. C.; Farkas, O.; Malick, D. K.; Rabuck, A. D.; Raghavachari, K.; Foresman, J. B.; Ortiz, J. V.; Cui, Q.; Baboul, A. G.; Clifford, S.; Cioslowski, J.; Stefanov, B. B.; Liu, G.; Liashenko, A.; Piskorz, P.; Komaromi, I.; Martin, R. L.; Fox, D. J.; Keith, T.; Al-Laham, M. A.; Peng, C. Y.; Nanayakkara, A.; Challacombe, M.; Gill, P. M. W.; Johnson, B.; Chen, W.; Wong, M. W.; Gonzalez, C.; Pople, J. A.; *Gaussian03*, Revision E.01; Gaussian, Inc: Wallingford, CT, 2004.

Table 2. Reaction Enthalpies and Free Energies (kcal/mol and 298 K) of LiH and NaH Cluster at the CCSD(T)/6-311++G(3d,2p)//MP2/6-311++G(2d,p) Level

decomposition	ΔG	ΔH	decomposition	ΔG	ΔH
$(LiH)_2 \rightarrow LiH + LiH$	37.5	46.4	$(NaH)_2 \rightarrow NaH + NaH$	27.6	36.3
$(LiH)_4 \rightarrow (LiH)_2 + (LiH)_2$	34.1	46.4	$(NaH)_4 \rightarrow (NaH)_2 + (NaH)_2$	28.4	40.5
$(LiH)_6 \rightarrow (LiH)_4 + (LiH)_2$	34.0	44.3	$(NaH)_6 \rightarrow (NaH)_4 + (NaH)_2$	30.2	40.0
$(LiH)_8 \rightarrow (LiH)_4 + (LiH)_4$	30.0	39.5	$(NaH)_8 \rightarrow (NaH)_4 + (NaH)_4$	29.0	38.3
$(LiH)_8 \rightarrow (LiH)_6 + (LiH)_2$	30.0	41.7	$(NaH)_8 \rightarrow (NaH)_6 + (NaH)_2$	27.2	48.7
$(LiH)_{10} \rightarrow (LiH)_6 + (LiH)_4$	27.0	36.5			
$(LiH)_{10} \rightarrow (LiH)_8 + (LiH)_2$	31.4	41.3			

$NaNH_2BH_3$, has a smaller total weight capacity (7.5 wt %) than $LiNH_2BH_3$ (10.9 wt %) under the same conditions.

$$NH_3BH_3(s) + LiH(s) \rightarrow LiNH_2BH_3(s) + H_2(g) \quad (1)$$

The nature of solid NH_3BH_3 and LiH are very different. In NH_3BH_3 the intermolecular interactions (dispersion plus dihydrogen bonding) are much weaker than in solid LiH where the ionic interactions result in an experimental lattice energy of 217.9 kcal/mol.[33] Morrison and Siddick[34] used a PW-DFT method to calculate a sublimation energy NH_3BH_3 of 18.2 kcal/mol. More recently, Matus et al.[35] determined an experimental value of 25 ± 3 kcal/mol for the sublimation of NH_3BH_3 from extrapolated vapor pressure data to 298 K. Such a large molecular cohesive energy of NH_3BH_3 is consistent with the low vapor pressure observed for solid NH_3BH_3, < 1 μm at ambient temperature.[36] Thus, sublimation of NH_3BH_3 is not expected in $LiNH_2BH_3$ formation and dehydrogenation. Furthermore, NH_3BH_3/LiH can also undergo dehydrogenation in THF solvent to form $LiNH_2BH_3$ and further dehydrogenation to form [LiN≡BH].[37] The activation barrier of dehydrogenation from LiH/NH_3BH_3 in this study[37] (11.1 kcal/mol) is in excellent accord with our calculated value (see below, $\Delta H^{\ddagger}$ = 12.4 kcal/mol, **1→TS1/3**).

The cohesion of LiH clusters up to $(LiH)_{10}$ was computed (Table 2) to determined the binding of smaller LiH units within a larger cluster. It was found that sublimation of small LiH cluster will not be involved in $LiNH_2BH_3$ formation since the dissociation energy is at least 35.5 kcal/mol ($(LiH)_{10} \rightarrow (LiH)_6 + (LiH)_4$). However, we suggest that the $(LiH)_4$ cluster unit may represent a useful model of the activated surface of the LiH crystal. Several ab initio calculations have shown that the cubic $(LiH)_4$ (T_d symmetry) is the most stable LiH cluster.[38]

If the reaction of NH_3BH_3 and LiH takes place through solid-to-solid contact, the most likely path is through the transfer of one NH_3BH_3 unit to the surface of the LiH crystal. Indeed, the calculated adsorption enthalpy (ΔH(298 K)) of NH_3BH_3 on the $(LiH)_4$ cluster is 17.1 kcal/mol (Figure 1 and eq 2) which largely compensates the sublimation energy[35] of NH_3BH_3 (25 ± 3 kcal/mol). The $(LiH)_4 \cdot NH_3BH_3$ complex (**1**) has a small 11.0 kcal/mol free energy barrier ($\Delta G^{\ddagger}$) to formation of the $(LiH)_3 \cdot LiNH_2BH_3$ complex (**3** + H_2) through **TS1/3**. A larger cluster model ($(LiH)_8$ rather than $(LiH)_4$) was tested for the reactions presented in Figure 1 and found to yield (at the B3LYP/6-31G(d) level) nearly the same energies (Supporting Information, Figure S1).

$$(LiH)_4 + NH_3BH_3 \rightarrow (LiH)_4 \cdot NH_3BH_3\ (\mathbf{1}) \rightarrow (LiH)_3 \cdot LiNH_2BH_3\ (\mathbf{3}) + H_2 \quad (2)$$

Since dehydrogenation of NH_3BH_3 has also been observed with NaH powder, the reaction profile was also calculated for $(NaH)_4$ + NH_3BH_3 in Figure 1 ($\Delta G(\Delta H)$ values given in brackets). In $(NaH)_4$, the free energy barrier is about half of $(LiH)_4$ (**1 → TS1/3**; $\Delta G^{\ddagger}$ = 5.5 versus 11.0 kcal/mol) which may be due to weaker Na−H (relative to Li−H) bonding. The electron-donating power of alkali metal is critical to promote amidoborane formation. This interpretation is confirmed by a study of MgH_2/NH_3BH_3 where the lower ionicity of MgH_2 reduces the strength of the $H^{\delta-} \cdots H^{\delta+}$ Coulombic attraction such that Mg^{2+}-substituted derivative of NH_3BH_3 are not observed.[39]

An alternative pathway to **3** involves initial cleavage of the N−B bond where the enthalpic barrier (**1 → TS1/2 → 2**) is 22.2 kcal/mol, slightly smaller than the N−B dative bond dissociation energy (27.5 ± 0.5 kcal/mol).[40] The product, $NH_3 \cdot (LiH_4)_4 \cdot BH_3$ (**2**) is significantly more stable than **1** ($\Delta G = -24.4$ kcal/mol). Given the four similar bond lengths around boron, **2** could also be viewed as a salt between $[NH_3 \cdot Li_4H_3]^+$ and $[BH_4]^-$. If **2** were formed from **1**, dehydrogenation would be much more difficult because the free energy barrier from **2 → 3** + H_2 is 45.3 kcal/mol.

Wu et al.[41] described the reaction of NH_3BH_3/LiH as a competition between H^- and $NH_2BH_3^-$. Hydride is a stronger base than $NH_2BH_3^-$ which is demonstrated by the free energy change of −24.4 kcal/mol for the reaction **1 → 3** + $\mathbf{H_2}$. Thus, the N−B bond dissociation mechanism for dehydrogenation from LiH/NH_3BH_3 through **TS1/2** and **TS2/3·H_2** cannot compete with dehydrogenation through the **TS1/3** without N−B bond dissociation. A key to avoiding borazine formation comes from the much lower activation barrier of **TS1/3** than direct H_2 elimination from NH_3BH_3. If initial dehydrogenation occurred first, as suggested from previous work on isolated NH_3BH_3,[42] then subsequent formation of borazine from NH_2BH_2 could not be avoided. Autrey and

(33) Rioux, F. *J. Chem. Educ.* **1977**, *54*, 555.
(34) Morrison, C. A.; Siddick, M. M. *Angew. Chem., Int. Ed.* **2004**, *116*, 4884.
(35) Matus, M. H.; Anderson, K. D.; Camaioni, D. M.; Autrey, T.; Dixon, D. A. *J. Phys. Chem.* **2007**, *111*, 4411.
(36) Alton, E. R.; Brown, R. D.; Carter, J. C.; Taylor, R. C. *J. Am. Chem. Soc.* **1959**, *81*, 3550.
(37) Xiong, Z.; Chua, Y. S.; Wu, G.; Xu, W.; Chen, P.; Shaw, W.; Karkamkar, A.; Linehan, J.; Smurthwaite, T.; Autry, T. *Chem. Commun.* **2008**, 5595.
(38) (a) Wang, X.; Andrews, L. *J. Phys. Chem. A* **2007**, *111*, 6008. (b) Bertolus, M.; Brenner, V.; Millie, P. *J. Chem. Phys.* **2001**, *115*, 4070. (c) Kato, H.; Hirao, K.; Nishida, I.; Kimoto, K.; Akagi, K. *J. Phys. Chem.* **1981**, *85*, 3391. (d) Kato, H.; Hirao, K.; Akagi, K. *Inorg. Chem.* **1981**, *20*, 3659.
(39) Kang, X.; Ma, L.; Fang, Z; Gao, L.; Luo, J.; Wang, S.; Wang, P. *Phys. Chem. Chem. Phys.* **2009**, *11*, 2507.
(40) Plumley, J. A.; Evanseck, J. D. *J. Chem. Theory Comput.* **2008**, *4*, 1249.
(41) Wu, H.; Zhou, W.; Yildirim, T. *J. Am. Chem. Soc.* **2008**, *130*, 14834.
(42) Stephens, F. H.; Pons, V.; Baker, R. T. *Dalton Trans.* **2007**, *25*, 2613.

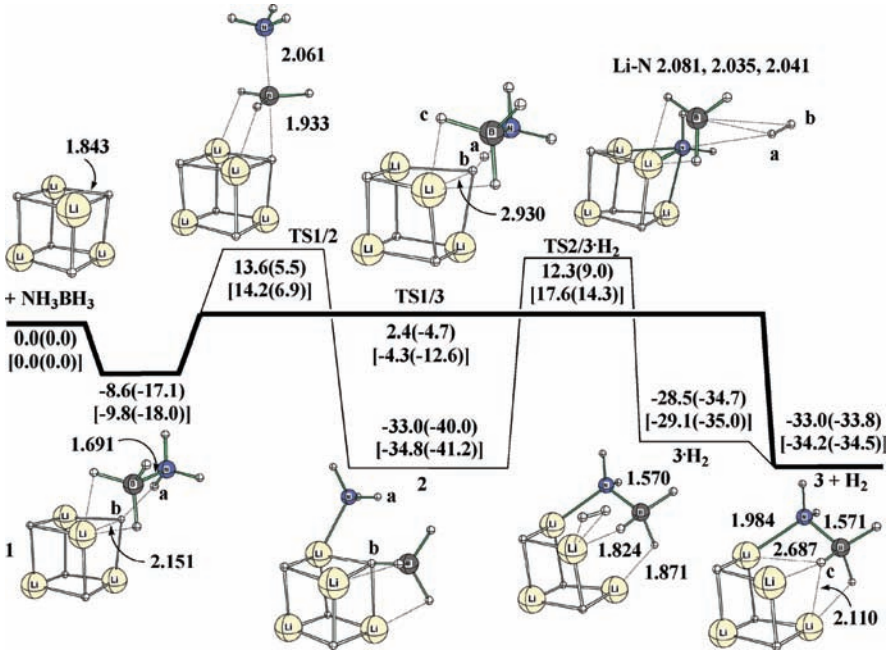

Figure 1. Free energy surface for the reaction of $(LiH)_4$ + NH_3BH_3. Free energies (kcal/mol) are relative to $(LiH)_4$ + NH_3BH_3 at 298 K. The values in parentheses are relative enthalpy (kcal/mol) to $(LiH)_4$ + NH_3BH_3 at 298 K. The values in bracket are free energies and enthalpies for the $(NaH)_4$ + NH_3BH_3 reaction pathway. Distances are in units of Angstroms.

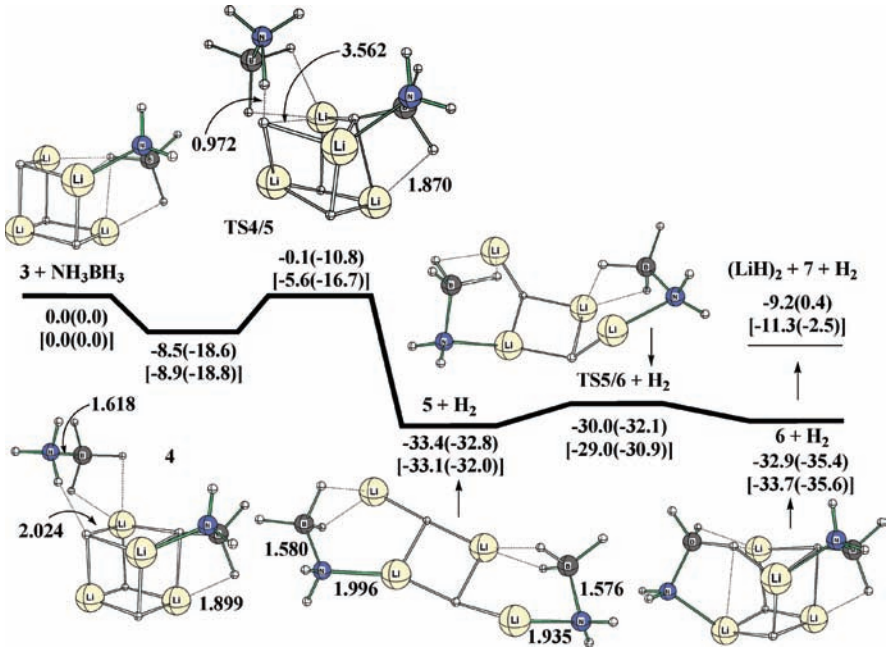

Figure 2. Free energy surface for the reaction of $(LiH)_3 \cdot LiNH_2BH_3$ (**3**) + NH_3BH_3.

co-workers[43,44] used NMR analysis to propose a decomposition mechanism of NH_3BH_3 in the solid state and solution through the formation of $[NH_3BH_2NH_3]^+[BH_4]^-$, the so-called DADB (diammoniate of diborane). On the basis of their studies, a pathway of dehydrogenation from DADB cannot avoid the formation of cyclic borazine in both solution and solid. In the present mechanism, BH_4^- and NH_2BH_2 intermediates are not formed, rather H_2 is formed through the recombination of a Lewis acid/base pair. A Li−N distance of 1.984 Å in **3** agrees well with the distance in solid $LiNH_2BH_3$ (2.032 Å), and a shortened N−B distance of 1.571 Å in **3** (Figure 1) agrees well with the distance in solid $LiNH_2BH_3$ (1.561 Å).[41]

The formation of a second $LiNH_2BH_3$ follows the same mechanism as the previous one, that is, **3** + NH_3BH_3 → **6** + H_2 (Figure 2), but with a lower free energy barrier for $H^{\delta-}\cdots H^{\delta+}$ formation in **TS4/5** (**4** → **TS4/5**, $\Delta G^{\ddagger}$ = 8.4 kcal/mol) relative to **TS1/3** (**1** → **TS1/3**, $\Delta G^{\ddagger}$ = 11.0 kcal/mol). The product of dehydrogenation, **5**, has a

(43) Stowe, A. C.; Shaw, W. J.; Linehan, J. C.; Schmid, B.; Autrey, T. *Phys. Chem. Chem. Phys.* **2007**, *9*, 1831.
(44) Shaw, W. J.; Linehan, J. C.; Szymczak, N. K.; Heldebrant, D. J.; Yonker, C.; Camaioni, D. M.; Baker, R. T.; Autrey, T. *Angew. Chem., Int. Ed.* **2008**, *47*, 7493.

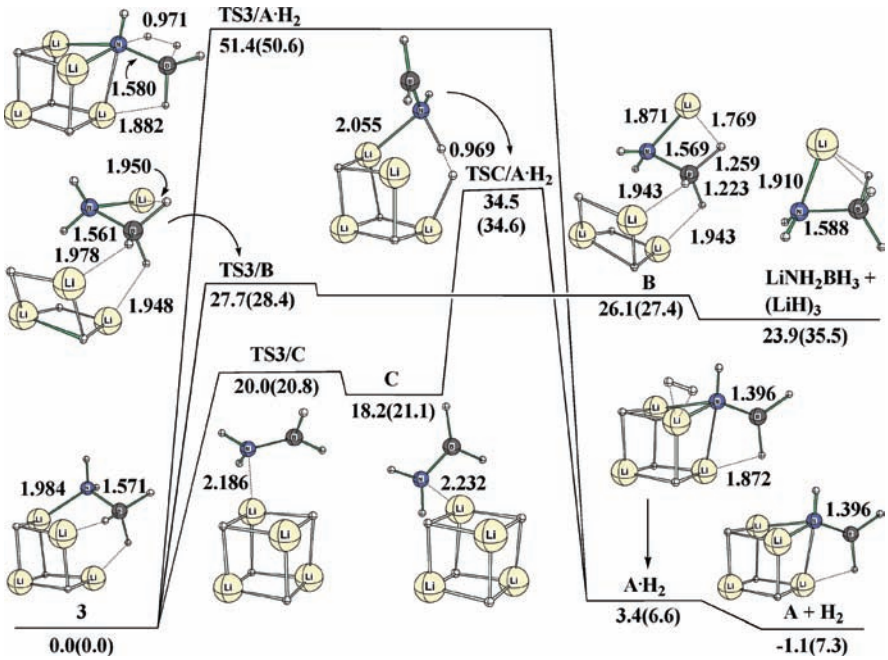

Figure 3. Comparison of free energy surface of **3** for dehydrogenation and formation of $LiNH_2BH_3$ + H_2.

rather flat Li−H network with a very small free energy barrier (**5** + $\mathbf{H_2}$ → **TS5/6** + $\mathbf{H_2}$, $\Delta G^{\ddagger}$ = 3.4 kcal/mol) to a more cube-like structure (**6** + $\mathbf{H_2}$). Reaction of $(NaH)_4$ with a second NH_3BH_3 molecule follows the same mechanism as for $(LiH)_4$ ($\Delta G(\Delta H)$ values for $(NaH)_4$ given in brackets in Figure 2) but with a smaller free energy barrier **4** → **TS4/5** ($\Delta G^{\ddagger}$ = 3.3 kcal/mol) compared to $(LiH)_4$ ($\Delta G^{\ddagger}$ = 8.4 kcal/mol). Thus, the free energy barrier for H_2 elimination from the addition of both NH_3BH_3 molecules to $(NaH)_4$ is about one-half that to $(LiH)_4$. However, the reaction of NaH with NH_3BH_3 is almost explosive, while that of LiH with NH_3BH_3 takes about 4 h for a complete reaction.[24] The lattice energy of NaH is 186.9 kcal/mol, which is not significantly smaller than LiH (217.9 kcal/mol[33]). However, the mechanical strength difference between NaH and LiH may be a factor for the difference in kinetics since NaH has a smaller bulk modulus compared to that of LiH (19.4 versus 32.2 GPa, respectively).[45,46] In addition, since the ball-milling process involves mechanical activation without solvent, the greater brittleness of NaH and low activation barrier may be a sufficient explanation for the large difference in reaction kinetics.

One can understand **3** as a cation−anion bound complex of $[Li_4H_3]^+[NH_2BH_3]^-$ where the LiH distance (2.687 Å) clearly shows disruption of cubic LiH (Figure 1). This LiH bond-breaking enables the detachment of $LiNH_2BH_3$ from the LiH cluster as described in Figure 3 (**3** → **TS3/B** → **B** → $LiNH_2BH_3$ + $(LiH)_3$). The transition state for elimination of $LiNH_2BH_3$ **TS3/B** is reached by rotating the NH_2Li group 180° around the N−B bond to form eclipsed $LiNH_2BH_3$ complexed with the $(LiH)_3$ cluster, **B**. The final geometry of the $(LiH)_3$ cluster has D_{3h} symmetry as previously reported.[38] However, this process is very endergonic, and the free energy barrier to **TS3/B** from **3** ($\Delta G^{\ddagger}$ = 27.7 kcal/mol) is much higher than the free energy barrier to **TS4/5** from **4** ($\Delta G^{\ddagger}$ = 8.4 kcal/mol) after the second NH_3BH_3 adsorption (Figure 2). Therefore, dissociation of $LiNH_2BH_3$ from the crystal is not likely. The possibility of concerted dehydrogenation from the N−B bond of **3** was also investigated, but the free energy barrier to H_2 release via **TS3/A·H₂** was much too high ($\Delta G^{\ddagger}$ = 51.4 kcal/mol) to be competitive. A mechanism through the intermediate **C** (**3** → **TS3/C** → **C** → **TSC/A·H₂** → **A·H₂**) was also considered but the free energy barrier from **3** to **TSC/A·H₂** ($\Delta G^{\ddagger}$ = 34.5 kcal/mol) is still too large to compete with addition and dehydrogenation of another NH_3BH_3 (**4** → **TS4/5**, $\Delta G^{\ddagger}$ = 8.4 kcal/mol). Thus, the formation of multiple $LiNH_2BH_3$ units on $(LiH)_4$ is much more favorable than concerted dehydrogenation from a single $LiNH_2BH_3$ on $(LiH)_4$, which explains why the $LiNH_2BH_3$ crystal is formed during the dehydrogenation experiment.

A major issue of hydrogen storage is its reversibility. For ammonia borane the first dehydrogenation is exothermic by 6.1 kcal/mol in the gas phase (Table 3). Miranda and Ceder[4] used DFT with solid-state modeling to calculate that the reaction was also exothermic in the solid solid state by 10 kcal/mol. Wu et al.[41] reported that dehydrogenation of $LiNH_2BH_3$ was not reversible while Kang et al.[26] reported the dehydrogenation reaction enthalpy was less exothermic than neat NH_3BH_3. However, to date, all the efforts for restoring the hydride (NH_3BH_3 + LiH) have failed.[24,26,41,47] In the present mechanism, $LiNH_2BH_3$ formation is exergonic for the first two steps step, $(LiH)_4$ + NH_3BH_3 → **3** + H_2 and **3** + NH_3BH_3 → **6** + H_2 (Figures 1 and 2, ΔG = −33.0 and −32.9 kcal/mol, respectively). The corresponding steps are slightly more exergonic for $(NaH)_4$ than $(LiH)_4$

(45) Loubeyre, P.; Le Toullec, R.; Hanfland, M.; Ulivi, L.; Datchi, F.; Hausermann, D. *Phys. Rev. B* **1998**, *57*, 10403.
(46) Duclos, S. J.; Vohra, Y. K.; Ruoff, A. L.; Filipek, S.; Baranowski, B. *Phys. Rev. B* **1987**, *36*, 7664.
(47) For a recent study of restoring the hydrogen capacity of a depleted hydride, see: Davis, B. L.; Dixon, D. A.; Garner, E. B.; Gordon, J. C.; Matus, M. H.; Scott, B.; Stephens F. H. *Angew. Chem., Int. Ed.* **2009**, ASAP.

Table 3. Reaction Enthalpies and Free Energies (kcal/mol and 298 K) of Aminoborane Oligomers at the CCSD(T)/6-311++G(3d,2p)//MP2/6-311++G(2d,p) Level

Equation	TS		Reaction	
	$\Delta G^{\ddagger}$	$\Delta H^{\ddagger}$	ΔG	ΔH
$NH_3{-}BH_3 \longrightarrow H_2N{=}BH_2 + H_2$	37.6	38.0	−15.0	−6.1
$H_2N{=}BH_2 \longrightarrow HN{\equiv}BH + H_2$	74.2	74.0	23.1	31.0
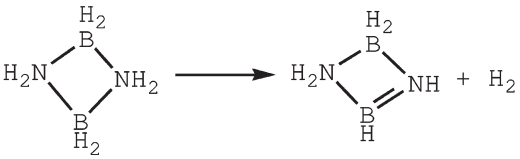	62.8	63.0	9.6	18.4
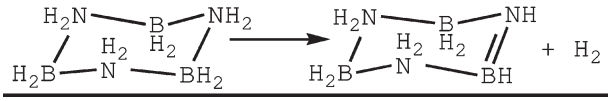	54.4	54.9	1.9	11.4

(ΔG = −34.2 and −33.7 kcal/mol, respectively). Thus, given the large exergonic/exothermic nature of the NH_3BH_3 + $(LiH)_4 \rightarrow LiNH_2BH_3 + H_2$ reaction, its reversibility is even more difficult than for $NH_3BH_3 \rightarrow NH_2BH_2 + H_2$. Bowden et al.[48] studied hydrogen generation from the methyl derivative. A recent theoretical study showed that $CH_3NH_2BH_3$ does not enhance dehydrogenation but does improve reversibility.[49]

For the catalytic dehydrogenation of NH_3BH_3, Ni-$(NHC)_2$ activated, Ruthenium catalyzed,[50,51] and Lewis acid BH_3 catalyzed dehydrogenations are known.[25] Ionic liquid also catalyzes dehydrogenation of NH_3BH_3.[52] However, these systems do not show increased hydrogen generation from NH_2BH_2. Another dehydrogenation pathway (eq 3), using gaseous NH_3 and LiH, was calculated to have an activation barrier of $\Delta H^{\ddagger}$ = 16.3 kcal/mol at the CCSD(T) level.[15] This pathway will be unpractical because of the energy requirements to sublime LiH units from the LiH crystal (Table 2). Comparing with the activation barrier between LiH/NH_3 ($\Delta H^{\ddagger}$ = 16.3 kcal/mol) and $(LiH)_4$/NH_3BH_3 (Figure 1, $\Delta H^{\ddagger}$ = 12.4 kcal/mol), the latter is lower than the former.

$$LiH(g) + NH_3(g) \rightarrow LiNH_2(g) + H_2(g) \qquad (3)$$

Chen et al.[9a] found 7 wt % reversible hydrogen storage using $LiNH_2(s)$ + LiH(s) but the operation condition of this dehydrogenation requires over 200 °C temperature. The authors proposed a polar mechanism with the formation of an $LiNH_2 \cdot LiH$ intermediate. Aguey-Zinsou et al.[16] also investigated the $LiNH_2$/LiH system and detected the existence of $Li_2NH_2^+$ and a penta-coordinated nitrogen Li_2NH_3 as intermediates by using thermal analysis and FTIR. The loss of H_2 from $(LiH)_n \cdot LiNH_2$ can be compared to the free energy barrier of $(LiH)_3 \cdot LiNH_2BH_3$ (**3**) to **TSC/A·H₂** (Figure 3, 34.5 kcal/mol) where the large barrier explains the high temperature need for the reaction.

Several studies of the $LiNH_2/LiBH_4$ solid state system have appeared including dehydrogenation.[53−56] In general, hydrogen storage systems involving $LiBH_4$ have a bottleneck because of its high thermal stability. At the standard level of theory in this study, the free energy for $LiBH_4$ decomposition (51.6 kcal/mol) shows why it is not easy to dehydrogenate (eq 4). Purewal et al.[57] suggested a combination of ScH_2 and $LiBH_4$ for

$$LiBH_4 \rightarrow LiH + BH_3$$
$$\Delta G = 51.6 \text{ kcal/mol (298 K)} \qquad (4)$$

hydrogen storage but, while the operation temperature is over 450 °C, they do observe that $LiBH_4$ decomposes into LiH as the final desorption product. Thus, dehydrogenation cannot easily occur if $LiBH_4$ is formed.

The existence of the Lewis acid BH_3 is critical to eliminate H with a low activation barrier. Thus, for $(LiH)_3 \cdot LiNH_2BH_3$ (**3**), in the first step Li^+ acts as relay agent to transfer a hydride from BH_3 to the LiH cluster (Figure 3, **3** → **TS3/C** → **C**), while in the second step (**C** → **TSC/A·H₂** → **A·H₂**) the hydride combines with the acidic proton on nitrogen to form H_2. A corresponding mechanism for $(LiH)_3 \cdot LiNH_2$ would not be possible because a hydride cannot be transferred.

Recently, Hügle et al.[58] reported that a mixture of hydrazine borane ($NH_2NH_2BH_3$) and LiH generated 12 wt % of H_2 at 150 °C (three H_2 molecules from $N_2H_4BH_3$/LiH mixture, which has 15.0 wt % hydrogen in total) without an induction period. The dehydrogenation behavior of hydrazine borane may be enhanced by LiH, which enables the formation of $Li^+(N_2H_3BH_3^-)$. However, the more rapid kinetics of the $N_2H_4BH_3$/LiH mixture may be related to the weak cohesive energy in the $N_2H_4BH_3$ lattice since the melting point of $N_2H_4BH_3$ lower than in NH_3BH_3 (61 and 110 °C,[23] respectively). The initial addition of $NH_2NH_2BH_3$ to $(LiH)_4$ and elimination of H_2 follow the same mechanism

(48) Bowden, M. E.; Brown, I. W. M.; Gainsford, G. J.; Wong, H. *Inorg. Chim. Acta* **2008**, *361*, 2147.
(49) Sun, C.-H.; Yao, X.-D.; Du, A.-J.; Li, L.; Smith, S.; Lu, G.-Q. *Phys. Chem. Chem. Phys.* **2008**, *10*, 6104.
(50) Yang, X.; Hall, M. B. *J. Am. Chem. Soc.* **2008**, *130*, 1798.
(51) Blaquiere, N.; Diallo-Garcia, S.; Gorelsky, S. I.; Black, D. A.; Fagnou, K. *J. Am. Chem. Soc.* **2008**, *130*, 14034.
(52) Bluhm, M. E.; Bradley, M. G.; Butterick, R. III; Kusari, U.; Sneddon, L. G. *J. Am. Chem. Soc.* **2006**, *128*, 7748.
(53) Noritake, T.; Aoki, M.; Towata, S.; Ninomiya, A.; Nakamori, Y.; Orimo, S. *Appl. Phys. A: Mater. Sci. Process.* **2006**, *83*, 277.
(54) Chater, P. A.; David, W. I. F.; Johnson, S. R.; Edwards, P. P.; Anderson, P. A. *Chem. Commun.* **2006**, *23*, 2439.
(55) Chater, P. A.; David, W. I. F.; Anderson, P. A. *Chem. Commun.* **2007**, *45*, 4770.
(56) Siegel, D.; Wolverton, C. *Phys. Rev. B* **2007**, *75*, 014101.
(57) Purewal, J.; Hwang, S.-J.; Bowman, R. C.; Rönnebro, E.; Fultz, B.; Ahn, C. *J. Phys. Chem. C* **2008**, *112*, 8481.
(58) Hügle, T.; Kühnel, M. F.; Lentz, D. *J. Am. Chem. Soc.* **2009**, *131*, 7444.

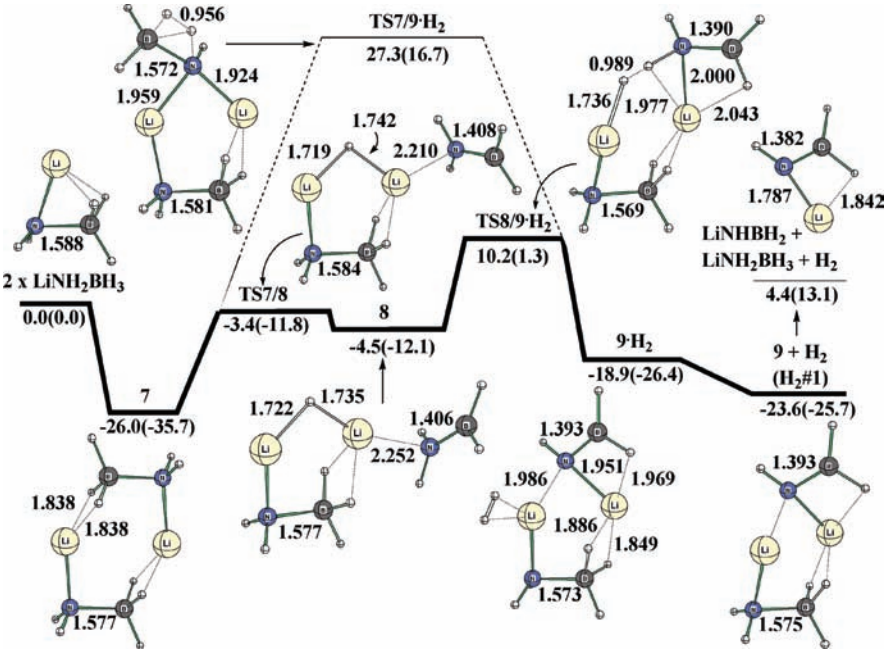

Figure 4. Dehydrogenation from a complex of two $LiNH_2BH_3$ molecules (**7**).

as NH_3BH_3 except that the H_2 elimination step has a lower free energy barrier ($\Delta G^{\ddagger} = 1.1$ kcal/mol at B3LYP/6-31G(d), see the Supporting Information, Figure S2)

The complex of two $LiNH_2BH_3$ molecules (**7**) resembles $LiBH_2NH_3$ in the crystal where two interacting Li^+ cations and hydrogen from BH_3 are in a zigzag arrangement.[41] In the crystal, the distances between Li and hydrogen of BH_3 are 1.976 Å and 2.116 Å while the corresponding distances in **7** (C_{2h} symmetry) are 1.838 Å. The interaction between two $LiNH_2BH_3$ units is very strong as shown in eq 5a where the intermolecular Li−H distance is 1.838 Å (Figure 4), which is shorter than that of $(LiH)_4$ cluster (Figure 1).

$$2LiNH_2BH_3 \rightarrow c\text{-}(LiNH{=}BH_2)_2\ (\mathbf{7}) \qquad \Delta G = -26.0\ \text{kcal/mol} \tag{5a}$$

$$c\text{-}(LiNH_2BH_3)_2\ (\mathbf{7}) \rightarrow LiNH_2BH_3 + NH_2BH_2 + LiH \tag{5b}$$

$$LiNH_2BH_3 + NH_2BH_2 + LiH \rightarrow Li_2N_2B_2H_8\ (\mathbf{9}) + H_2 \quad (H_2\#1) \tag{5c}$$

To get one mole of H_2 from $LiNH_2BH_3$, two H_2 molecules should be generated from the $LiNH_2BH_3$ dimer.[59] The first dehydrogenation mechanism is summarized as shown in eqs 5b and 5c (H_2#1 indicates the first H_2 molecule generated from $(LiNH_2BH_3)_2$ dimer; later steps generate H_2#2, H_2#3, and H_2#4). However, one-step dehydrogenation through **TS7/9·H$_2$** is very unfavorable (**7** → **TS7/9·H$_2$** → **9·H$_2$**, $\Delta G^{\ddagger} = 53.3$ kcal/mol) compared to a two-step mechanism (**7** → **TS7/8** → **8** → **TS8/9·H$_2$** → **9·H$_2$**, $\Delta G^{\ddagger} = 36.2$ kcal/mol) (Figure 4). One may compare this enthalpy barrier ($\Delta H^{\ddagger} = 37.0$ kcal/mol) of the two-step mechanism with the first dehydrogenation from NH_3BH_3, which is $\Delta H^{\ddagger} = 33.8$ kcal/mol at CCSD(T)/CBS level[27] or $\Delta H^{\ddagger} = 36.4$ kcal/mol at DFT.[60] However, the sublimation enthalpy of the NH_3BH_3 crystal (25 ± 3 kcal/mol) should be added to the NH_3BH_3 dehydrogenation barrier to make a fair comparison since **7** represents solid $LiNH_2BH_3$. Nguyen et al.[30] report the dehydrogenation enthalpy barrier of 44.5 to 59.4 kcal/mol for $(NH_3BH_3)_2$, which exhibits the same topology as **7**. Thus, the first dehydrogenation of $LiNH_2BH_3$ through a two-step mechanism is lower than dehydrogenation of NH_3BH_3.

A N−B bond distance of 1.572 Å in **TS7/9·H$_2$** indicates single-bond character. However, the N−B bond distances in **TS7/8** and **TS8/9·H$_2$** are 1.408 Å and 1.390 Å, which indicate double-bond character. The formation of a Li−H−Li bridge in **TS7/8** weakens one of the Li−N bonds in one $LiNH_2BH_3$ unit where NH_2BH_2 is bound to the Li^+ cation in **8**. Breaking a Li−H bond (1.735 → 2.470 Å) and forming a H−H bond (0.989 Å) in **TS8/9·H$_2$** enables dehydrogenation and formation of the complex **9·H$_2$**. This two-step mechanism (**7** → **8** → **9·H$_2$**) lowers the free energy barrier by 17.1 kcal/mol when compared with the one-step dehydrogenation. The first dehydrogenation product, a complex of $LiNH_2BH_3$ and $LiNH{=}BH_2$ **9**, has stronger intermolecular interactions than in the complex of two $LiNH_2BH_3$ molecules **7** (**7** → 2x$LiNH_2BH_3$, $\Delta G = -26.0$ kcal/mol and **9** + H_2 → $LiNH{=}BH_2$ + $LiNH_2BH_3$ + H_2, $\Delta G = -28.0$ kcal/mol, respectively).

The second dehydrogenation of $LiNH_2BH_3$ starting from **9** follows the formation of a Li−H−Li bridge in **TS9/10** (Figure 5) where NH_2BH_2 is again bound to the Li^+ cation in **10**. Thus, the second dehydrogenation (loss of H_2#2) from **9** (**9** → **10** → **11**, eq 6a) follows the same pathway as the previous dehydrogenation (**7** → **8** → **9**, eq 5b) using Li^+ as a relay agent for hydride. The enthalpic dehydrogenation barrier from **9** to **TS10/11·H$_2$** ($\Delta H^{\ddagger} = 40.5$ kcal/mol) is still lower than for $(NH_3BH_3)_2$. The dehydrogenation of

(59) While we consider the $(LiNH_2BH_3)_2$ dimer as the minimum reactive species of solid $LiNH_2BH_3$, the minimum unit may be larger, i.e., trimer or tetramer.

(60) Nutt, W. R.; McKee, M. L. *Inorg. Chem.* **2007**, *46*, 7633.

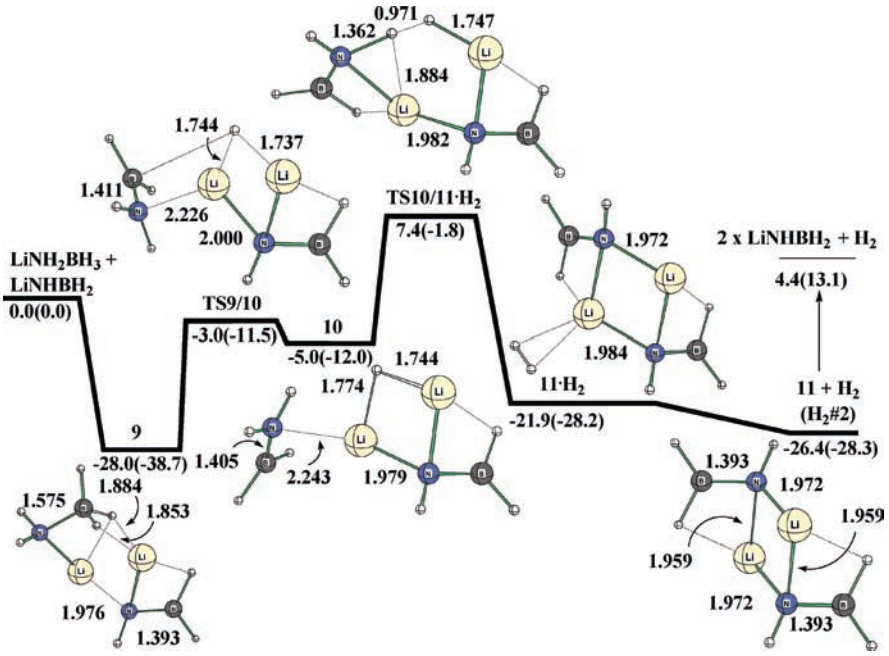

Figure 5. Dehydrogenation from a complex of $LiNH_2BH_3$ and $LiNH{=}BH_2$ molecules (**9**).

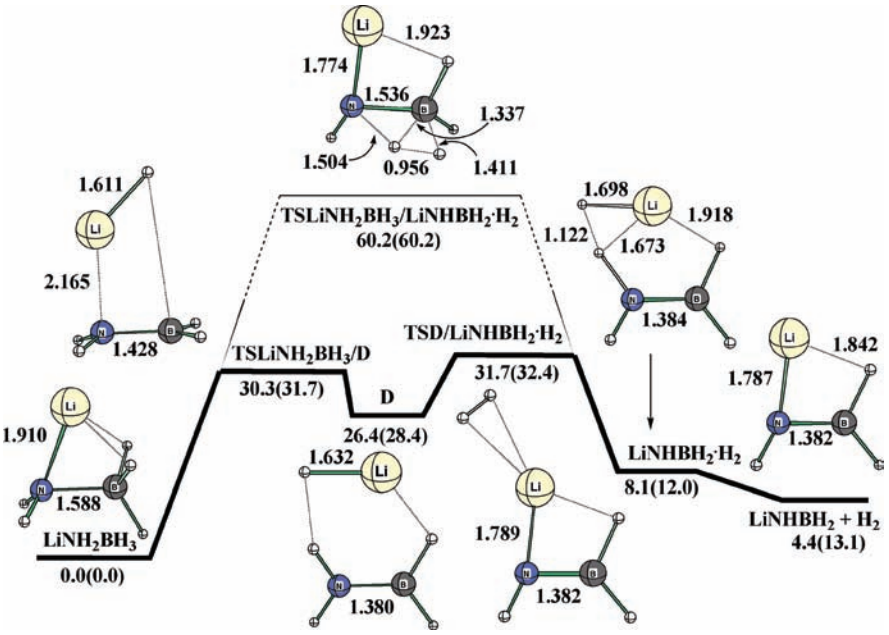

Figure 6. One-step dehydrogenation (**TSLiNH$_2$BH$_3$/LiNHBH$_2$·H$_2$**) and a two-step dehydrogenation (**TSLiNH$_2$BH$_3$/D → D → TSD/LiNHBH$_2$·H$_2$**) pathway of a single $LiNH_2BH_3$ molecule.

$LiNH_2BH_3$ is slightly endergonic, (ΔG = 2.4 kcal/mol **7** → **9** + H_2, Figure 4 and ΔG = 1.6 kcal/mol **9** → **11** + H_2, Figure 5) while the dehydrogenation from $(LiH)_4$ and NH_3BH_3 is very exergonic (ΔG = −33.0 kcal/mol **1**→ **3** + H_2, Figure 1 and ΔG = −32.9 kcal/mol **3** + NH_3BH_3 → 6 + H_2, Figure 2). The final product of dehydrogenation from the $LiNH_2BH_3$ complex, **11**, is a complex between two $LiNH{=}BH_2$ units with a square Li−N network and two N=B double bonds. One may observe the strengthened intermolecular interactions between two units in the complexes **7**, **9**, and **11** (ΔG = −26.0, −28.0, and −30.8 kcal/mol, respectively) as H_2 is released. The complex **11** (C_i symmetry) requires further rearrangement to achieve dehydrogenation (loss of H_2#3 and H_2#4) since the Li^+ cation in the Li−N network is not free to act as a relay agent for hydride.

$$Li_2N_2B_2H_8\ (\mathbf{9}) \rightarrow LiNH{=}BH_2 + NH_2BH_2 + LiH \quad (6a)$$

$$\begin{aligned} &LiNH{=}BH_2 + NH_2BH_2 \\ &\quad + LiH \rightarrow c\text{-}(LiNH{=}BH_2)_2\ (\mathbf{11}) \\ &\quad + H_2 \qquad (H_2\#2) \end{aligned} \quad (6b)$$

Before proceeding to the third dehydrogenation (loss of H_2#3) from **11**, it is valuable to compare dehydrogenation from a single $LiNH_2BH_3$ molecule (eq 5 and Figure 6) to

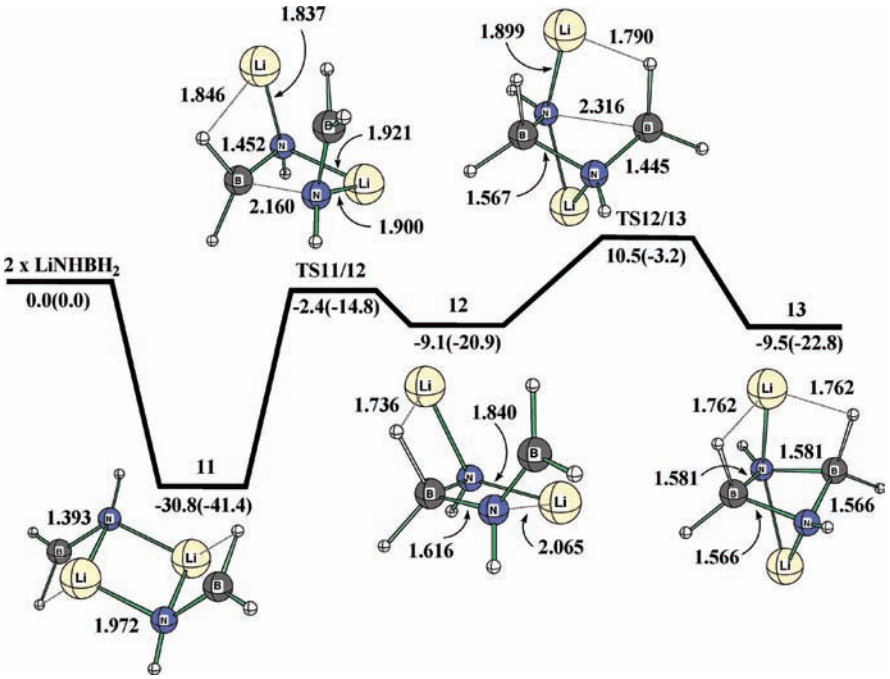

Figure 7. Rearrangement process of a $(LiNH{=}BH_2)_2$ complex (**11**).

form $LiNH{=}BH_2$ as a final product. The one-step dehydrogenation through **TSLiNH$_2$BH$_3$/LiNHBH$_2$·H$_2$** has a very unfavorable free energy barrier ($\Delta G^{\ddagger} = 60.2$ kcal/mol) with a N−B single bond distance (1.536 Å) and **LiNH$_2$BH$_3$ → LiNH$_2$BH$_2$** + H_2 shows slight endergonic nature (ΔG = 4.4 kcal/mol, Figure 6). The two-step dehydrogenation occurs with a lower free energy barrier (**LiNH$_2$BH$_3$ → TSLiNH$_2$BH$_3$/D → D → TSD/LiNHBH$_2$·H$_2$ → LiNHBH$_2$** + H_2, $\Delta G^{\ddagger}$ = 30.3 kcal/mol) than the one-step dehydrogenation and is analogous to the two-step dehydrogenation of **7** to **9** ($\Delta G^{\ddagger}$ = 29.4 kcal/mol, Figure 4). Therefore, dehydrogenation of $LiNH_2BH_3$ is not promoted by the formation of $(LiNH_2BH_3)_2$ dimer but by the Li^+ relay (Li−H−Li moiety) mechanism. Staubitz et al.[3] showed that dimerization of ammoniaborane were reduced when functional groups such as methyl are added to nitrogen.

The rearrangement of **11** (eq 7) starts by replacing a Li−N bond by a N−B bond as shown in **TS11/12** and **12** (Figure 7). The Li^+ cation can make a strong Li−H interaction with the hydrogen of the BH_2 group in **TS11/12** (1.846 Å), which is similar to the Li−H distances in the $(LiH)_4$ cluster (1.843 Å). The second Li−N interaction is replaced by a N−B bond in a reaction requiring 19.6 kcal/mol in free energy (**12** → **TS12/13**) which is smaller than the first Li−N → N−B replacement (ΔG = 28.4 kcal/mol, **11** → **TS11/12**). The relatively small free energy barrier is possible because of two interactions of the Li^+ cation with nitrogen and a strong LiH bond (1.790 Å) in **TS12/13**. In the final cyclic N−B bonded complex (**13**), the N−B bond lengths are 1.566 Å and 1.581 Å (Figure 7).

$$c\text{-}(LiNH{=}BH_2)_2 \rightarrow Li_2N_2B_2H_6 \qquad (7)$$

It should be pointed out that the reaction of **11**→**13** is strongly endergonic (21.3 kcal/mol) which suggests that the Li^+ cation movement in the $LiNH{=}BH_2$ bulk matrix is disfavored. The final dehydrogenation generates amorphous LiN≡BH with one mole of H_2 released (eq 8).[24]

$$LiNH{=}BH_2(s) \rightarrow LiNBH(s) + H_2(g) \qquad (8)$$

The reaction of two $LiNH{=}BH_2$ units (**13**) may follow a similar pathway as the reaction of two $LiNH_2BH_3$ units as shown in eq 9a and eq 9b.

$$Li_2N_2B_2H_6\ (\mathbf{13}) \rightarrow LiN_2B_2H_5 + LiH \qquad (9a)$$

$$LiN_2B_2H_5 + LiH \rightarrow Li_2N_2B_2H_4\ (\mathbf{15}) + H_2 \quad (H_2\#3) \qquad (9b)$$

In the pathway **13** → **15**, the role of Li^+ as a relay agent for hydride can be recognized. The Li^+ cation in **TS13/14** abstracts a hydride from one BH_2 group and interacts with a hydrogen atom of the other BH_2 group while the N−B bond in **14** shortens (1.566 → 1.442 Å) because of rehybridization ($sp^3 \rightarrow sp^2$) around boron. As hydride is relayed in **TS14/15·H$_2$**, the LiH unit swings around to abstract a H^+ from nitrogen to form the product complex **15·H$_2$** where H_2 is coordinated to lithium. The final product **15** has a Li^+ cation coordinated to two nitrogen atoms and one hydrogen atom of the BH_2 group (Figure 8). The dehydrogenation process for H_2#3 shows a very endergonic nature (**11** → **15** + H_2, ΔG = 28.5 kcal/mol) while dehydrogenation steps of H_2#1 and H_2#2 are almost thermoneutral.

A discrepancy between two experimental studies[24,26] (Table 1) involves release of H_2#3 and H_2#4 in the NH_3BH_3/Li system. On the basis of the observation from Kang et al.,[26] 10.4 wt % of H_2 release is available after 2.5 h at 120 °C or after 5 h at 100 °C. However, an additional 0.8H_2 equiv (total 14.5 wt % of H_2 from NH_3BH_3/LiH) is only available at 200 °C which corresponds to all of H_2#3 and

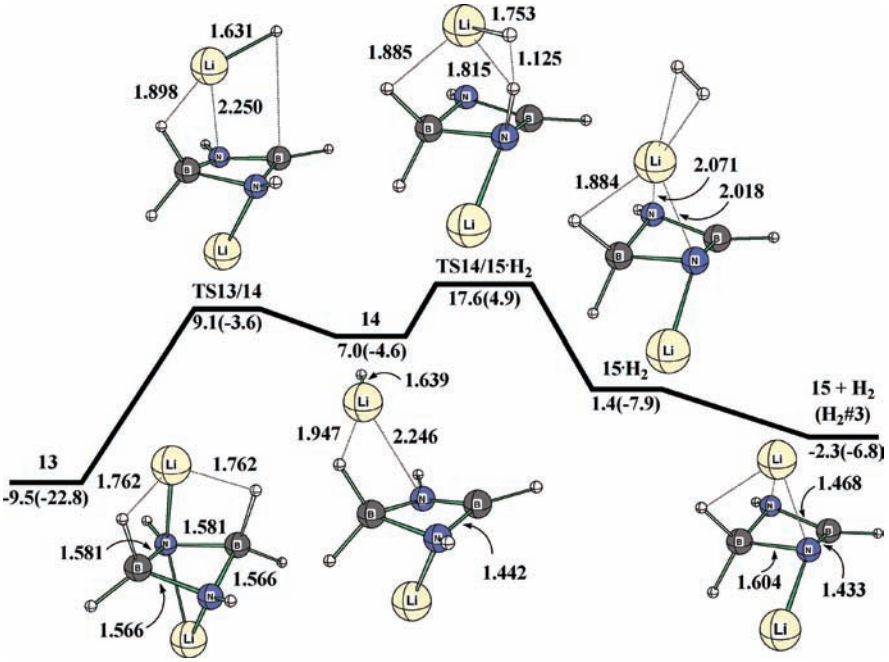

Figure 8. Dehydrogenation of a $(LiNH{=}BH_2)_2$ complex (**13**).

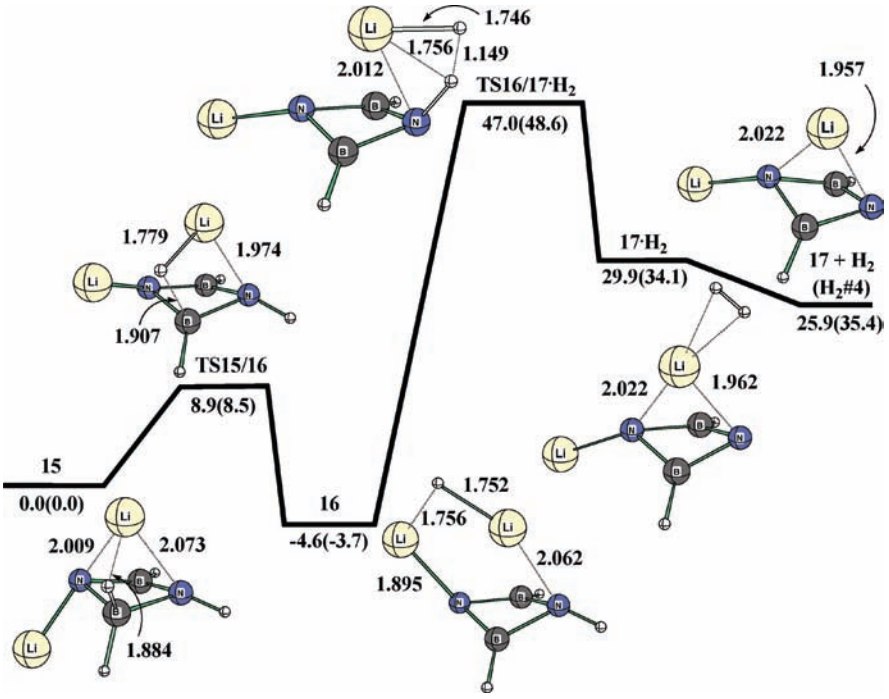

Figure 9. Dehydrogenation of $Li_2N_2B_2H_4$ (**15**).

partial H_2#4. The fourth H_2 (H_2#4) is essential to achieve over 10 wt % of H_2 from $LiNH_2BH_3$ in our calculations since dehydrogenation of H_2#1, H_2#2, and H_2#3 is 8.4 wt % from $(LiNH_2BH_3)_2$. To achieve one molar equivalent dehydrogenation (loss of H_2#3) from eq 9b, one more H_2 molecule should be available from $Li_2N_2B_2H_6$ (Figure 9). Dehydrogenation (loss of H_2#4) of **16** is very difficult ($\Delta G^{\ddagger} = 51.6$ kcal/mol) where the Li^+ relay agent transfers a hydride from boron to nitrogen to form the product complex **17·H$_2$**. The distances between the Li^+ cation and nitrogen in **TS16/17·H$_2$** are 2.012 Å and 2.407 Å (2.407 Å is not shown explicitly in **TS16/17·H$_2$**). The two-step reaction eq 10a and eq 10b summarizes the second dehydrogenation (loss of H_2#4) from $Li_2N_2B_2H_4$ (**18**).

$$Li_2N_2B_2H_4\ (\mathbf{15}) \rightarrow LiN_2B_2H_3 + LiH\ (\mathbf{16}) \qquad (10a)$$

$$LiN_2B_2H_3 + LiH\ (\mathbf{16}) \rightarrow Li_2N_2B_2H_2\ (\mathbf{17}) + H_2\ (H_2\#4) \qquad (10b)$$

While high, the free energy barrier **16** → **TS16/17·H$_2$** ($\Delta G^{\ddagger}$ = 51.6 kcal/mol) is still significantly lower than the barrier $NH_2BH_2 \rightarrow HN{\equiv}BH + H_2$ ($\Delta G^{\ddagger}$ = 74.2 kcal/mol).

Table 4. Reaction Enthalpies and Free Energies (kcal/mol and 298 K) for Each Step at the CCSD(T)/6-311++G(3d2p)//MP2/6-311++G(2d,p) Level

dehydrogenation	equation	TS		reaction	
		$\Delta G^{\ddagger}$	$\Delta H^{\ddagger}$	ΔG	ΔH
$NH_3BH_3 + (LiH)_4 \rightarrow LiNH_2BH_3 + H_2$	**1**→ **TS1/3**→**3** + H_2	11.0	12.4	−24.4	−16.7
	4→ **TS4/5**→**5** + H_2	8.4	7.8	−24.9	−14.2
	5 + H_2→ **TS5/6** + H_2→**6** + H_2	3.4	0.7	0.5	−2.6
$LiNH_2BH_3 \rightarrow LiNH{=}BH_2 + H_2$	**7**→ **TS7/8**→**8**	22.6	23.9	21.5	23.6
	8→ **TS8/9**→**9** + H_2	14.7	13.4	−19.1	−13.6
	9→ **TS9/10**→**10**	25.0	27.2	23.0	26.7
	10→**TS10/11**→**11** + H_2	12.4	10.2	−21.4	−16.3
$LiNH{=}BH_2 \rightarrow LiN{\equiv}BH + H_2$	**11**→ **TS11/12**→**12**	28.4	26.6	21.7	20.5
	12→ **TS12/13**→**13**	19.6	17.7	−0.4	−1.9
	13→**TS13/14**→ **14**	18.6	19.2	16.5	18.2
	14→**TS14/15**→**15** + H_2	10.6	9.5	−9.3	−2.2
	15→**TS15/16**→**16**	8.9	8.5	−4.6	−3.7
	16→**TS26/17**→**17** + H_2	51.6	52.3	30.5	39.1

Table 5. Atomic Charges from Natural Bond Orbital Analysis at the MP2/6-11++G(2d,p) Level

$NH_3{-}BH_3$	B	−0.12	$LiNH_2{-}BH_3$	B	−0.16
	N	−0.83		N	−1.13
				Li	0.84
$NH_2{=}BH_2$	B	0.45	$LiNH{=}BH_2$	B	0.30
	N	−1.00		N	−1.21
				Li	0.84
$HN{\equiv}BH$	B	0.63	$LiN{\equiv}BH$	B	0.51
	N	−0.97		N	−1.34
				Li	0.92

Thus, dehydrogenation of NH_2BH_2, $N_2B_2H_8$, *c*-$N_3B_3H_{12}$ have much higher free energy barriers than **13** → **TS14/15·H$_2$** ($\Delta G^{\ddagger}$ = 27.2 kcal/mol) and **16** → **TS16/17·H$_2$** ($\Delta G^{\ddagger}$ = 51.6 kcal/mol). Li et al.[61] studied several structures of $H(H_2N{=}BH_2)_nH$ oligomers but did not investigate the dehydrogenation mechanism for the hydrogen storage application. In experiments by Xiong et al., about 8 wt % of hydrogen is released within 1 h, which would corresponding to the release of H_2#1, H_2#2, and H_2#3 from $(LiNH_2BH_3)_2$ which gives 8.2 wt %. After 19 h 3 additional wt % of hydrogen is released which would correspond to release of H_2#4 from $(LiNH_2BH_3)_2$ (2.7 additional wt %).[24] Both the increasing free energy barriers and the endergonic nature of late dehydrogenation steps explain the early saturation and the slow kinetics of subsequent $LiNH_2BH_3$ dehydrogenation.

One concern is the unfavorable pathway between **15** and **17** + H_2 (Figure 9) since it becomes more strongly endothermic (ΔH = 35.4 kcal/mol, Table 4) than a pathway between **11** and **15** + H_2 (ΔH = 34.6 kcal/mol, Table 4). From the report of Miranda and Ceder,[4] dehydrogenation from NH_3BH_3 is exothermic in both the gas-phase (ΔH = −5.7 kcal/mol)[2] and solid-state (ΔH = −1.6 kcal/mol) while dehydrogenation from NH_2BH_2 is strongly endothermic in the gas-phase (30.3 kcal/mol) but exothermic in the solid-state (−9.6 kcal/mol). In addition, recent experimental thermal analysis shows a distinct two-step exothermic decomposition accompanied by the generation of 2.2 mol H_2/mol from NH_3BH_3 powder.[62] Therefore, hydrogen loss from solid-state NH_2BH_2 has a significant enthalpy contribution from lattice stabilization of the product, amounting to as much as 39.9 kcal/mol (30.3 + 9.6). Such an increase in lattice stabilization is not found in the dehydrogenation of NH_3BH_3. However, lattice stabilization of $LiNH_2BH_3$ and products of its dehydrogenation might be stronger than those of NH_3BH_3 because of the ionic character of $LiNH_2BH_3$ and its dehydrogenation products (Table 5). If one assumes that hydrogen loss from $LiNH_2BH_3$ and $LiNH{=}BH_2$ would roughly parallel that from NH_3BH_3 and NH_2BH_2, the energetics of hydrogen loss from $LiNH{=}BH_2$ might be seriously underestimated. As a very crude estimate of free energy changes for hydrogen loss in the solid-state from $(LiNH{=}BH_2)_2$ (about 40 kcal/mol), we will decrease the free energy change for loss of H_2#3 and H_2#4 by 20 kcal/mol for each step (Table 6). Thus, loss of H_2#1 (**7** → **9** + H_2) and H_2#2 (**9** → **11** + H_2) is nearly thermoneutral, while H_2#3 would be thermoneutral if increased lattice energy stabilization was included. Thus, the three initial H_2-loss steps are consistent with rapid evolution of 8 wt % of hydrogen.[24] Loss of H_2#4 has a more unfavorable free energy/enthalpy change (ΔH = 70.0−40 kcal/mol ΔG = 54.4−40 kcal/mol) and, while observed, the evolution of 3 additional wt % is much slower.

During the revision process of this article, a quantum mechanical study for the dehydrogenation mechanism for loss of H_2#1 and H_2#2 from $LiNH_2BH_3$ based on the $(LiNH_2BH_3)_2$ unit (**7**) was published by Kim et al.[63] They identified two mechanism for loss of H_2#1 and H_2#2, the "L" pathway which corresponds to the mechanism in our manuscript, and the "L*" pathway, a new mechanism where a new N−B bond is formed before the loss of H_2#1. We have recomputed all of the transition states and intermediates in their "L" and "L*" pathways at our standard level of theory and have extended the "L*" pathway to include elimination of H_2#3 (Figure 10). The "L" pathway corresponds to our Li^+ relay mechanism (Li−H−Li moiety) and is consistent with our mechanism between **7** to **11** + H_2 with minor differences in geometry in **1′**, **T1t**, **T2h**, and **4t** (their notation). Their enthalpy values for reaction pathway "L" agree with our values to within about 2 kcal/mol except for **11** (**5H$_2$** in their notation) which we calculate to be 20.6 kcal/mol less stable than **7** $(LiNH_2BH_3)_2$ while they report **5H$_2$** (their notation) is 30.3 kcal/mol less stable than $(LiNH_2BH_3)_2$ (**1** in their notation). In terms of enthalpy, pathway "L*" is slightly more favorable than pathway "L" but **TS8/9·H$_2$** (Pathway L) and **T5h** (Pathway L*) are within 0.6 kcal/mol

(61) Li, J.; Kathmann, S. M.; Schenter, G. K.; Gutowski, M. *J. Phys. Chem. C* **2007**, *111*, 3294.

(62) Baitalow, F.; Baumann, J.; Wolf, G.; Jaenicke-Rößler, K.; Leitner, G. *Thermochim. Acta* **2002**, *391*, 159.

(63) Kim, D. Y.; Singh, N. J.; Lee, H. M.; Kim, K. S. *Chem.—Eur. J.* **2009**, *15*, 5598.

Table 6. Reaction Enthalpies and Free Energies (kcal/mol) for Each Step at the CCSD(T)/6-311++G(3d,2p)//MP2/6-311++G(2d,p) Level

	ΔG (298 K)	ΔG (365 K)[a]	DLS[b]	best estimate for solid $LiNH_2BH_3$ at ΔG (365 K)	ΔH (298 K)
7 → **9** + H_2	2.4	0.7	0.0	0.7	10.0
7 → **11** + $2H_2$	4.0	0.3	0.0	0.3	20.4
7 → **15** + $3H_2$	32.5	27.5	20.0[c]	7.5	55.0
7 → **17** + $4H_2$	58.4	51.2	40.0[d]	11.2	90.4
$NH_3BH_3 \rightarrow HN{\equiv}BH + 2H_2$	8.2	4.5			24.7
$LiNH_2BH_3 \rightarrow LiN{\equiv}BH + 2H_2$	21.7	17.8			39.1

[a] Experimental condition of ref [24]. [b] Differential Lattice energy Stabilization (see text). [c] The free energy change for the reaction in solid is increased by 20 kcal/mol because of the larger lattice energy of product-solid compared to the lattice energy of the reactant-solid. [d] The free energy change for the reaction in solid is increased by 20 kcal/mol relative to **15** + $3H_2$ to account for differential lattice energy stabilization. The total change with respect to **7** is 40 kcal/mol.

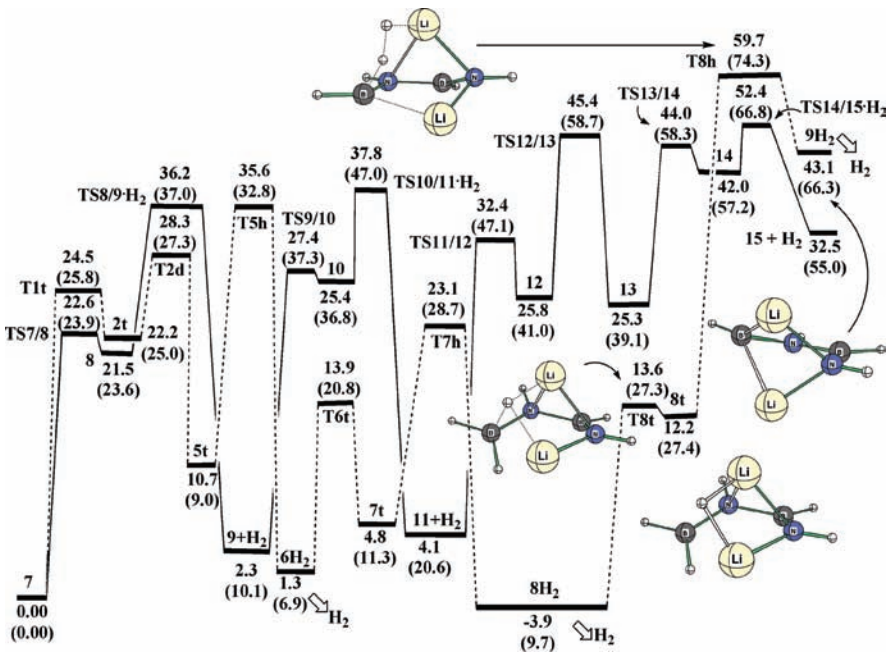

Figure 10. Free energy surface of dehydrogenation from $(LiNH_2BH_3)_2$ dimer (H_2#1, H_2#2, and H_2#3). Free energies and enthalpies (kcal/mol) are relative to **7** at 298 K. The values in parentheses are relative enthalpies (kcal/mol) to **7** at 298 K. Dotted lines represent pathway from ref [60].

in terms of free energy. A chain N−B bond is formed early in the "L*" pathway while a cyclic N−B bond is formed in the "L" pathway. Thus, this N−B bond chain formation might be a key to understand the difference from the two experimental studies[24,26] for H_2#3 and H_2#4 release from $(LiNH_2BH_3)_2$.

Conclusions

The formation of $LiNH_2BH_3$ crystal from $(LiH)_4$ + NH_3BH_3 and its stepwise dehydrogenation mechanism is investigated through an ab initio study. A competition mechanism between H^- and $NH_2BH_3^-$ is proposed to explain $LiNH_2BH_3$ formation during the ball-milling process. Exchange of the $NH_2BH_3^-$ and H^- positions is possible at the edge of cubic $(LiH)_4$ geometry, which represent the active surface of bulk LiH crystal. The dehydrogenation of $LiNH_2BH_3$ is facilitated by relaying a hydride from boron to Li^+, which then abstracts a H^+ from NH_3 to form H_2. Thus, Li^+ plays a key role by carrying the hydride from boron to nitrogen. The rearrangement of the $(LiNH{=}BH_2)_2$ complex to $Li_2N_2B_2H_6$, which requires the replacement of Li−N bonds by N−B bonds, is necessary for the third and fourth equimolecular dehydrogenation. If differential lattice energy effects in the dehydrogenation of $(LiNH_2BH_3)_2$ dimer are sufficiently large, the present results suggest that four molecules of H_2 from $(LiNH_2BH_3)_2$ dimer may be reversibly available, which corresponds to 10.9 wt % of hydrogen.

Acknowledgment. Computer time was made available on the Alabama Supercomputer Network.

Supporting Information Available: Table S1 gives total energies (hartrees), zero-point energies (kcal/mol), thermal corrections to 298 K (kcal/mol), and entropies (cal/mol·K) for all species shown in the Figures 1−10. Table S2 gives Cartesian coordinates of geometries optimized at the MP2/6-311++G(2d, p) level for all species shown in the Figures 1−10. Figure S1 presents the potential energy surface for the addition of NH_3BH_3 to $(LiH)_8$ at the B3LYP/6-31G(d) level. Figure S2 presents the potential energy surface for the addition of $NH_2NH_2BH_3$ to $(LiH)_4$ at the B3LYP/6-31G(d) level. This material is available free of charge via the Internet at http://pubs.acs.org.